doi:10.3772/j.issn.1006-6748.2019.02.003

Modeling and robust adaptive control for a coaxial twelve-rotor UAV①

Pei Xinbiao(裴信彪)* **, Peng Cheng②*, Bai Yue*, Wu Helong* **, Ma Ping* **
(* Changchun Institute of Optics, Fine Mechanics and Physics, Chinese Academy of Sciences, Changchun 130033, P. R. China)
(** University of Chinese Academy of Sciences, Beijing 100039, P. R. China)

Abstract

Compared with the quad-rotor unmanned aerial vehicle (UAV), the coaxial twelve-rotor UAV has stronger load carrying capacity, higher driving ability and stronger damage resistance. This paper focuses on its robust adaptive control. First, a mathematical model of a coaxial twelve-rotor is established. Aiming at the problem of model uncertainty and external disturbance of the coaxial twelve-rotor UAV, the attitude controller is innovatively adopted with the combination of a backstepping sliding mode controller (BSMC) and an adaptive radial basis function neural network (RBFNN). The BSMC combines the advantages of backstepping control and sliding mode control, which has a simple design process and strong robustness. The RBFNN as an uncertain observer, can effectively estimate the total uncertainty. Then the stability of the twelve-rotor UAV control system is proved by Lyapunov stability theorem. Finally, it is proved that the robust adaptive control strategy presented in this paper can overcome model uncertainty and external disturbance effectively through numerical simulation and prototype of twelve-rotor UAV tests.

Key words: coaxial twelve-rotor unmanned aerial vehicle (UAV), backstepping sliding mode controller (BSMC), adaptive radial basis function neural network (RBFNN), external disturbances

0 Introduction

In recent years, the quad-rotor unmanned aerial vehicle (UAV) has attracted people's attention because of its simple mechanical structure, flexible flight mode and excellent vertical take-off and landing capability[1]. It is widely used in aerial photography, patrol and information collection[2]. However, uncertainty in flight brings many problems with the control of the unmanned aerial vehicle[3]. Therefore, the robust adaptive control method of quad-rotor UAV with model uncertainty and external disturbance has gradually aroused people's attention. The model reference adaptive control technology[4] is used for the quad-rotor control under the uncertainty of model parameters. The effectiveness of the method is verified by the simulation of the dynamic mode of the battery, motor and sensor. Ryan et al[5] proposed a robust controller of quad-rotor dynamic external interference, a variety of uncertainties nonlinear cancellation and saturated integrator. A super twisting algorithm proposed in Ref. [6] was applied to a quad-rotor so as to ensure strong robustness against external disturbances. The fuzzy inference mechanism was designed to help estimating the upper bound of lumped uncertainties of quad-rotor[7].

The above robust control strategy is based on the inherent structure of the four rotor and has significant under actuated characteristics. Based on this situation a new type of coaxial twelve- rotor UAV is developed in this paper. The twelve rotors are divided into six groups, the rotation of the rotors in each group is opposite and is installed at the end of the six carbon fiber arms. The six groups of the rotor in the non-planar are able to provide independently adjusted forces and moments in the three axles. This unique design can eliminate the under actuated characteristic. In the meantime, the yaw attitude control ability is greatly improved due to the fact that the yaw movement provided by reactive torque in quad-rotor is replaced by the lift force in twelve-rotor. Therefore, the twelve-rotor UAV offers remarkable advantages including greater driving capability and better robustness against disturbances.

Considering the uncertainties and disturbances of the model, the design of the twelve-rotor attitude controller innovatively adopts the combination of BSMC

① Supported by the National Natural Science Foundation of China (No. 11372309, 61304017), Youth Innovation Promotion Association (No. 2014192), the Provincial Special Funds Project of Science and Technology Cooperation (No. 2017SYHZ0024), and the Key Technology Development Project of Jilin Province (No. 20150204074GX).

② To whom correspondence should be addressed. E-mail: litianjinorc@126.com

Received on May 6, 2018

and adaptive RBFNN. The BSMC has strong robustness to disturbances because of its insensitivity to disturbances, and the uncertainty observer of adaptive RBFNN can estimate the uncertainty of the model and accurately estimate the uncertainty range of external disturbances[8]. Finally, simulation results show that the BSMC with adaptive RBFNN has good attitude control performance under uncertain and time-varying external disturbances. Meanwhile, practicability of the proposed method applied to the coaxial twelve-rotor is corroborated by prototype experiments.

1 Dynamic model of coaxial twelve-rotor UAV

The structure of the coaxial twelve rotor UAV is shown in Fig. 1. The angle between the six arms is 60°, the rotor 1/3/5/8/10/12 counterclockwise rotates, the rotor 2/4/6/7/9/11 clockwise rotates, the angle between the rotating shaft and the body plane is γ degrees ($0 < \gamma < 20°$). Two references coordinates are defined to represent the dynamic characteristics of the twelve-rotor, that is, the earth-fixed inertial frame $E = \{Ox_e y_e z_e\}$ and the body-fixed frame $B = \{Ox_b y_b z_b\}$. Thrust f_i and reactive torque τ_i produced by the ith rotor are expressed as

$$\begin{aligned} f_i &= k_i \Omega_i^2 \\ \tau_i &= k_{\tau i} \Omega_i^2 \end{aligned} \tag{1}$$

where $i = 1, 2, \cdots, 12$ represents the rotor number, k_i and $k_{\tau i}$ are the thrust coefficient and reactive torque coefficient respectively, Ω_i expresses the ith rotor speed.

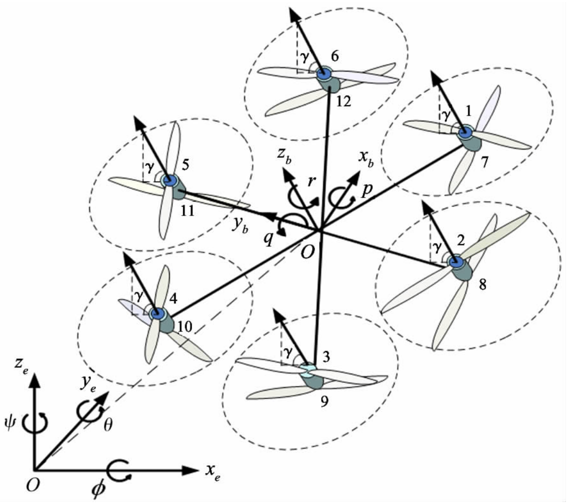

Fig. 1 The scheme of coaxial twelve-rotor UAV

The position vector $\boldsymbol{P}_i \in R^3$, $i = 1, 2, \cdots, 12$ of the ith rotor in body-fixed frame B is defined as follows:

$$\begin{aligned} \boldsymbol{P}_1 &= \boldsymbol{P}_7 = \begin{bmatrix} \frac{\sqrt{3}}{2} & -\frac{1}{2} & 0 \end{bmatrix}^{\mathrm{T}} \\ \boldsymbol{P}_2 &= \boldsymbol{P}_8 = [0 \quad -1 \quad 0]^{\mathrm{T}} \\ \boldsymbol{P}_3 &= \boldsymbol{P}_9 = \begin{bmatrix} -\frac{\sqrt{3}}{2} & -\frac{1}{2} & 0 \end{bmatrix}^{\mathrm{T}} \\ \boldsymbol{P}_4 &= \boldsymbol{P}_{10} = \begin{bmatrix} -\frac{\sqrt{3}}{2} & \frac{1}{2} & 0 \end{bmatrix}^{\mathrm{T}} \\ \boldsymbol{P}_5 &= \boldsymbol{P}_{11} = [0 \quad 1 \quad 0]^{\mathrm{T}} \\ \boldsymbol{P}_6 &= \boldsymbol{P}_{10} = \begin{bmatrix} \frac{\sqrt{3}}{2} & \frac{1}{2} & 0 \end{bmatrix}^{\mathrm{T}} \end{aligned} \tag{2}$$

The direction vector $\boldsymbol{D}_i \in R^3$, $i = 1, 2, \cdots 12$ of the ith rotor in body-fixed frame B is defined as follows

$$\begin{aligned} \boldsymbol{D}_1 &= \boldsymbol{D}_4 = \boldsymbol{D}_7 = \boldsymbol{D}_{10} = \begin{bmatrix} \frac{1}{2}\sin\gamma & \frac{\sqrt{3}}{2}\sin\gamma & \cos\gamma \end{bmatrix}^{\mathrm{T}} \\ \boldsymbol{D}_2 &= \boldsymbol{D}_5 = \boldsymbol{D}_8 = \boldsymbol{D}_{11} = [-\sin\gamma \quad 0 \quad \cos\gamma]^{\mathrm{T}} \\ \boldsymbol{D}_3 &= \boldsymbol{D}_6 = \boldsymbol{D}_9 = \boldsymbol{D}_{12} = \begin{bmatrix} \frac{1}{2}\sin\gamma & -\frac{\sqrt{3}}{2}\sin\gamma & \cos\gamma \end{bmatrix}^{\mathrm{T}} \end{aligned} \tag{3}$$

Then, resultant F in body-fixed frame B is written as

$$F = \sum_{i=1}^{12} (\boldsymbol{P}_i \cdot f_i) \tag{4}$$

and resultant moment M in the body-fixed frame B as

$$M = \sum_{i=1}^{12} (\boldsymbol{P}_i \times f_i l + \boldsymbol{D}_i \cdot \tau_i) \tag{5}$$

The twelve-rotor UAV is regarded as a symmetric rigid body of six degrees of freedom. The dynamic equation of the rotation of the center of mass can be obtained by the Newton-Euler formula as

$$(J + \Delta J) \cdot \dot{\omega} = -sk(\omega) \cdot (J + \Delta J) \cdot \omega + M \tag{6}$$

where $J = diag(I_x, I_y, I_z)$ is the moment of inertia, $\Delta J = diag(\Delta I_x, \Delta I_y, \Delta I_z)$ is the uncertainty of the inertia matrix caused by the change of the mass properties. $\omega = [p, q, r]^{\mathrm{T}}$ is the angle velocity. $\boldsymbol{sk}(\omega)$ as skew-symmetric matrix is denoted by

$$\boldsymbol{sk}(\omega) = \begin{bmatrix} 0 & -r & q \\ r & 0 & -p \\ -q & p & 0 \end{bmatrix} \tag{7}$$

Considering the external disturbance, the kinematic equations that rotate around the center of mass can be considered as

$$\begin{bmatrix} \ddot{\varphi} \\ \ddot{\theta} \\ \ddot{\psi} \end{bmatrix} = \begin{bmatrix} M_x/(I_x + \Delta I_x) + \tau_{dx} \\ M_y/(I_y + \Delta I_y) + \tau_{dy} \\ M_z/(I_z + \Delta I_z) + \tau_{dz} \end{bmatrix} \tag{8}$$

where $\tau_d = [\tau_{dx} \quad \tau_{dy} \quad \tau_{dy}]$ denotes external disturbances, Euler angles $\eta = [\varphi \quad \theta \quad \psi]^{\mathrm{T}}$ expresses the attitude angles and $M = [M_x \quad M_y \quad M_z]^{\mathrm{T}}$ represents the resultant moment.

The translational model using the Newton-Euler formulas is derived as

$$m\frac{\mathrm{d}V}{\mathrm{d}t} = m\left(\frac{\delta V}{\delta t} + \omega \times V\right) = F + \Delta F + \boldsymbol{R}^{-1}G \tag{9}$$

where $V = [u,\ v,\ w]^{\mathrm{T}}$ expresses the velocity with respect to B, ΔF is seen as the neglectful aerodynamic force. The rotation matrix map vector $\boldsymbol{R}$ from the body-fixed frame B to the inertial frame E is expressed as

$$\boldsymbol{R} = \begin{bmatrix} \cos\psi\cos\theta & -\sin\psi\cos\phi + \cos\psi\sin\theta\sin\phi & \sin\psi\sin\phi + \cos\psi\sin\theta\cos\phi \\ \sin\psi\cos\theta & \cos\psi\cos\phi + \cos\psi\sin\theta\sin\phi & -\cos\psi\sin\phi + \sin\psi\sin\theta\cos\phi \\ -\sin\theta & \cos\theta\sin\phi & \cos\theta\cos\phi \end{bmatrix} \tag{10}$$

Moreover, there is the relationship between inertial translational position $P = [x \quad y \quad z]^{\mathrm{T}}$ and velocity V as follows

$$\dot{P} = \boldsymbol{R} \cdot V \tag{11}$$

Therefore, the translational dynamic model of the twelve-rotor is given as:

$$\begin{bmatrix} \ddot{x} \\ \ddot{y} \\ \ddot{z} \end{bmatrix} = \frac{1}{m}\begin{bmatrix} F_x\cos\psi\cos\theta + F_y(\cos\psi\sin\theta\cos\phi - \sin\psi\cos\phi) \\ + F_z(\cos\psi\sin\theta\cos\phi + \sin\psi\sin\phi) \\ F_x\sin\psi\cos\theta + F_y(\cos\psi\sin\theta\sin\phi + \cos\psi\cos\phi) \\ + F_z(\sin\psi\sin\theta\cos\phi - \cos\psi\sin\phi) - F_x\sin\theta \\ + F_y\sin\varphi\cos\psi + F_z\cos\theta\cos\phi - mg \end{bmatrix} \tag{12}$$

2 Robust attitude control of twelve-rotor UAV

Taking into account the model uncertainties and external disturbances in attitude control of coaxial twelve-rotor UAV, the attitude controller is designed as a combination of BSMC and adaptive RBFNN. Fig. 2 describes the block diagram of the attitude controller of a coaxial twelve-rotor UAV, including three modules: roll, pitch and yaw modules. The three modules are all made up of BSMC and adaptive RBFNN.

Taking the roll module of UAV as an example:

$$\begin{aligned} \dot{x}_1 &= x_2 \\ \dot{x}_2 &= \frac{M_x}{I_x} + D_x \end{aligned} \tag{13}$$

where x_1 is the roll angle, x_2 is the roll angle velocity. $D_x = \tau_{dx} + f_x$ represents the total uncertainty of the roll module, $f_x = -\Delta I_x M_x / [(I_x + \Delta I_x) \cdot I_x]$ indicates the uncertainty of the module when τ_{dx} as the external disturbance is limited.

Firstly, the roll angle tracking error is defined as

$$z_1 = x_{1d} - x_1 \tag{14}$$

with x_{1d} as the desired roll angle. Define the stabilizing function as

$$c_1 = \alpha_1 z_1 \tag{15}$$

with α_1 as a positive constant value and $z_2 = x_2 - \dot{x}_{1d} - c_1$ is the speed tracking error of the roll angle. Choose the first Lyapunov function as $V_1 = z_1^2/2$, then the derivative of V_1 is

$$\dot{V}_1 = z_1(\dot{x}_{1d} - x_2) = -z_1 z_2 - \alpha z_1^2 \tag{16}$$

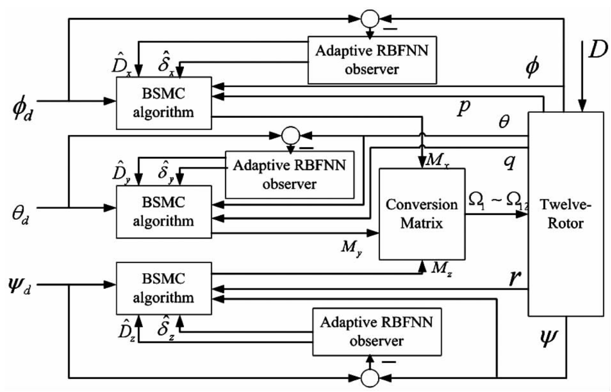

Fig. 2 The block diagram of the attitude controller of the twelve-rotor UAV

Due to the fact that the derivative of z_2 can be expressed as

$$\begin{aligned} \dot{z}_2 &= \dot{x}_2 - \ddot{x}_{1d} - \alpha\dot{z}_1 \\ &= M_x/I_x + D_x - \ddot{x}_{1d} + \alpha(z_2 + \alpha z_1) \end{aligned} \tag{17}$$

therefore, the second Lyapunov function is chosen by

$$V_2 = V_1 + \frac{1}{2}s^2 \tag{18}$$

and where

$$s = kz_1 + z_2 \tag{19}$$

with k is a positive constant. Thereby, it can be derived that

$$\begin{aligned} \dot{V}_2 &= \dot{V}_1 + s\dot{s} = -z_1 z_2 - \alpha z_1^2 + s(kz_1 + z_2) \\ &= -z_1 z_2 - \alpha z_1^2 + s[(k - \alpha)\dot{z}_1 + M_x/I_x + D_x - \ddot{x}_{1d}] \end{aligned} \tag{20}$$

Then, in an attempt to estimate lumped uncertainty D_x, an adaptive RBFNN observer is designed. The structure of the RBFNN is described in Fig. 3. Choosing the Gauss function as the receptive field function, the input vector is expressed as $Z = [z_1, \dot{z}_1]^{\mathrm{T}}$. The output based on the weighted sum method is taken as

$$\hat{D}_x = \sum_{j=1}^{N} W_j \varphi_j(Z) \quad j = 1, 2, \cdots, N \tag{21}$$

$$\phi_j(Z) = \exp(-|Z - M_j|^2/\sigma_j^2) \tag{22}$$

where W_j represents the weight between the hidden layer and the output layer. N represents the number of hidden nodes. Each hidden node includes the center vector described by M_j and the width described by σ_j.

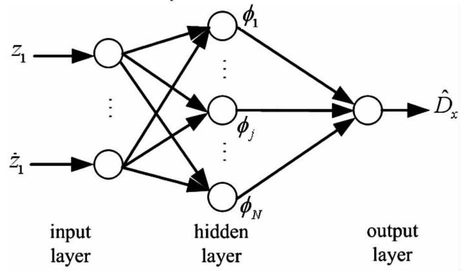

Fig. 3 The structure of RBFNN

The training process is divided into two steps, where the first step is unsupervised learning, and training determines center vector $\boldsymbol{M}_j$ and width σ_j, the second step is supervised learning, training determines weight W_j.

First, the training methods of the center vector $\boldsymbol{M}_j$ is taken as

$$\boldsymbol{M}_j = i_{\min} + \frac{i_{\max} - i_{\min}}{2N} + (j-1) \cdot \frac{i_{\max} - i_{\min}}{N} \tag{23}$$

where $i_{\min}$ is the minimum value of all input information for the ith feature, $j = 1, 2, \cdots, N$.

Then, training width vector affects the range of neurons' input information. The shape of the corresponding hidden layer function is narrower when the width is smaller, the less the information near the center of the neuron will respond to the neuron. The training method is designed by

$$\sigma_j = d_f \cdot \sqrt{\frac{1}{N} \cdot \sum_{j=1}^{N} Z - \boldsymbol{M}_j} \tag{24}$$

where d_f is the width adjustment coefficient, and the value is less than 1. The purpose is to make each hidden layer neuron easier to sense local information and improve the local response ability of RBFNN.

Finally, the training weights are given, and the detailed calculation method is given in combination with the output. Defining the minimum reconstructed error δ_x is taken as follows

$$\delta_x = D_x - \hat{D}_x(\boldsymbol{W}^*) \tag{25}$$

where $\boldsymbol{W}^*$ expresses an optimal weight vector. Then, it can be derived that

$$V_3 = V_2 + \frac{1}{2\eta_1}(\boldsymbol{W}^* - \boldsymbol{W})^{\mathrm{T}}(\boldsymbol{W}^* - \boldsymbol{W}) + \frac{1}{2\eta_2}(\delta_x - \hat{\delta}x)^2 \tag{26}$$

where η_1 and η_2 are both positive constants, $\hat{\delta}_x$ is the estimated value of δ_x. Then, the derivative of V_3 can be derived as

$$\begin{aligned} \dot{V}_3 &= V_2 - \frac{1}{\eta_1}(\boldsymbol{W}^* - \boldsymbol{W})^T \dot{W} - \frac{1}{\eta_2}(\delta_x - \delta_x)\dot{\delta}_x \\ &= -z_1 z_2 - \alpha z_1^2 + s[(k-\alpha)\dot{z}_1 + M_x/I_x + D_x - \ddot{x}_{1d}] \\ &\quad - \frac{1}{\eta_1}(\boldsymbol{W}^* - \boldsymbol{W})^T \dot{W} - \frac{1}{\eta_2}(\delta_x - \delta_x)\dot{\delta}_x \end{aligned} \tag{27}$$

Therefore, BSMC with RBFNN controller law U_x is designed by

$$\begin{aligned} U_x = M_x = I_x[&-(k-\alpha)\dot{z}_1 + \ddot{x}_{1d} - ws - h\operatorname{sgn}(s) \\ &- U_H - U_R] \end{aligned} \tag{28}$$

where w and h are both positive constants, U_H as the robust controller and U_R as the compensated controller are designed as follows respectively:

$$U_H = \hat{D}_x(W) \tag{29}$$

$$U_R = \hat{\delta}_x \tag{30}$$

Design adaptation laws for $\dot{W}$ and $\dot{\hat{\delta}}_x$ as follows:

$$\dot{W} = s\eta_1 \phi(X) \tag{31}$$

$$\dot{\hat{\delta}}_x = s\eta_2 \tag{32}$$

Then, it can be derived by

$$\dot{V}_3 = -z_1 z_2 - \alpha z_1^2 - ws^2 - h|s| \tag{33}$$

Therefore, the BSMC with adaptive RBFNN controller system is asymptotically stable in the case of $w(\alpha - k) - \frac{1}{4} > 0$. In the roll control module, BSMC and adaptive RBFNN method can guarantee the stability of the algorithm under the uncertainty of the model and the unknown external interference bounds. In addition, the pitch controlled module and the yaw control module use the same attitude control strategy, which is no longer described for the sake of simplicity.

3 Numerical simulation results

The simulation of the BSMC and adaptive RBFNN algorithm for the coaxial twelve-rotor UAV is carried out in the case of uncertainty and external disturbances. Table 1 is the dynamic model parameter of the twelve-rotor UAV.

Table 1 The parameters of the eight-rotor prototype

Parameters	Values
Mass m	4.45 kg
Distance between rotor and the centre l	0.5 m
Moment of inertia to x-axis I_x	2.6×10^{-2} N · m/s^2
Moment of inertia to y-axis I_y	2.6×10^{-2} N · m/s^2
Moment of inertia to z-axis I_z	4.2×10^{-2} N · m/s^2
Thrust factor k_1	54.2×10^{-6} N · s^2
Drag factor k_2	1.1×10^{-6} N · m/s^2

The initial attitude angles are assumed as $\eta_0 = [0 \quad 0 \quad 0]^{\mathrm{T}}$ degree, the desired attitude angles are set as $\eta_d = [12\cos(t) \quad 12\cos(t) \quad 20\cos(t)]^{\mathrm{T}}$ degree.

An uncertainty of -30% is given as the model uncertainties in the inertia matrix. Assume the time-varying external disturbance acting on the three attitudes as $\tau_d = 0.2\sin(0.5t)$. In addition, the relevant parameters of the BSMC algorithm are set as follows:

$\alpha_x = 11$, $k_x = 0.4$, $\gamma_x = 18$, $h_x = 1$, $\alpha_y = 14$, $k_y = 0.5$, $\gamma_y = 21$, $h_y = 3$, $\alpha_z = 12$, $k_z = 0.5$, $h_z = 1$

What's more, the number of hidden layer nodes of RBFNN is set to 6, which corresponds to six degrees of freedom model and twelve rotors divided into six groups. The center is set to 3 according to the flight attitude training sample, and the central value is fixed. The width of each hidden layer is 7, which is calculated according to Eq. (24). In addition, learning factors are set as $\eta_1 = 10$, $\eta_2 = 4$.

Fig. 4, Fig. 5 and Fig. 6 describe three attitude compared simulations separately under model uncertainties and time-varying external disturbance. It is clear

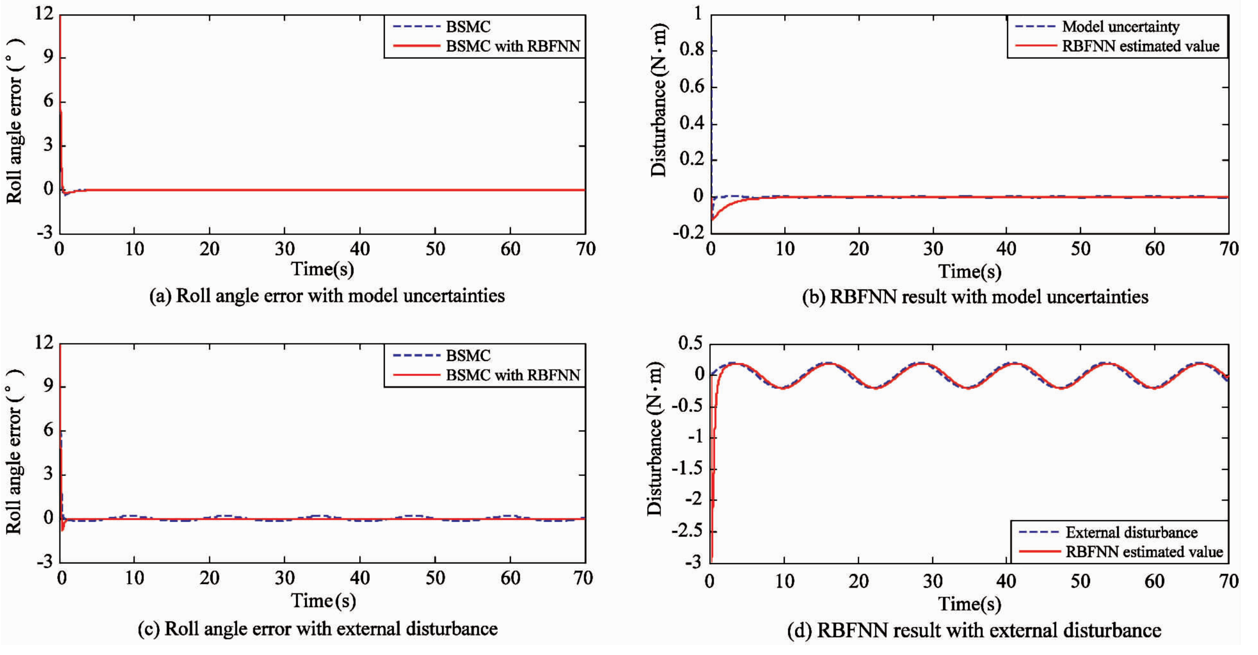

(a) Roll angle error with model uncertainties

(b) RBFNN result with model uncertainties

(c) Roll angle error with external disturbance

(d) RBFNN result with external disturbance

Fig. 4 The roll control result with uncertainties

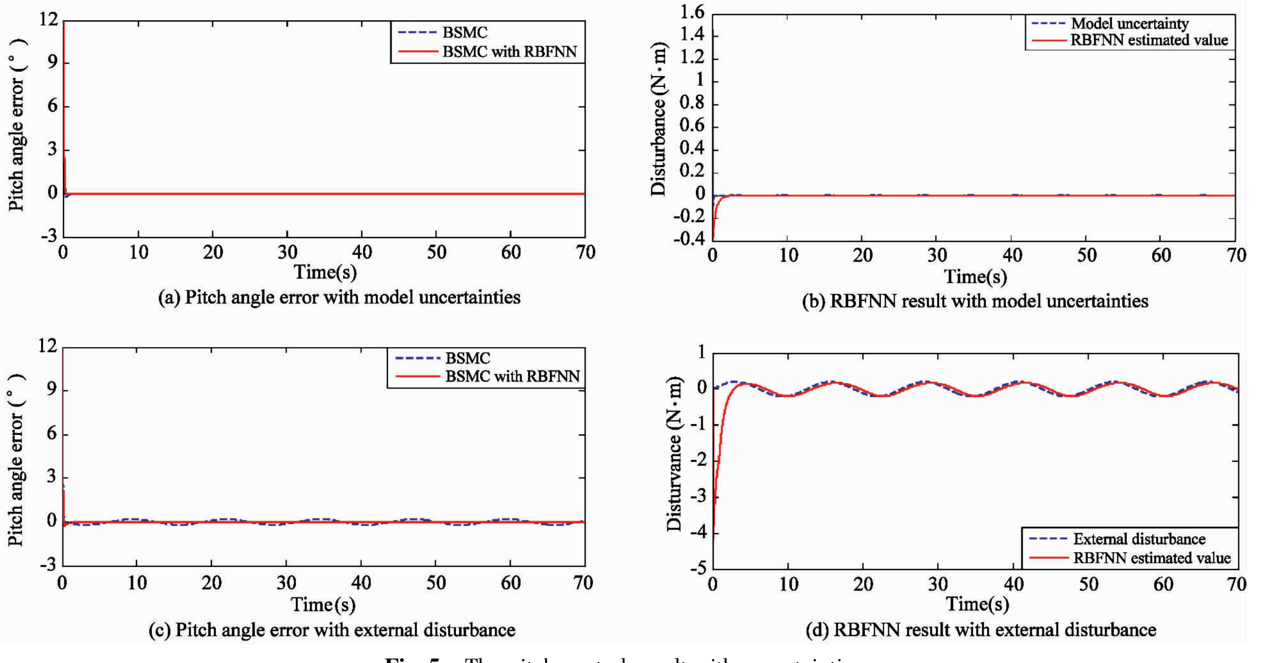

(a) Pitch angle error with model uncertainties

(b) RBFNN result with model uncertainties

(c) Pitch angle error with external disturbance

(d) RBFNN result with external disturbance

Fig. 5 The pitch control result with uncertainties

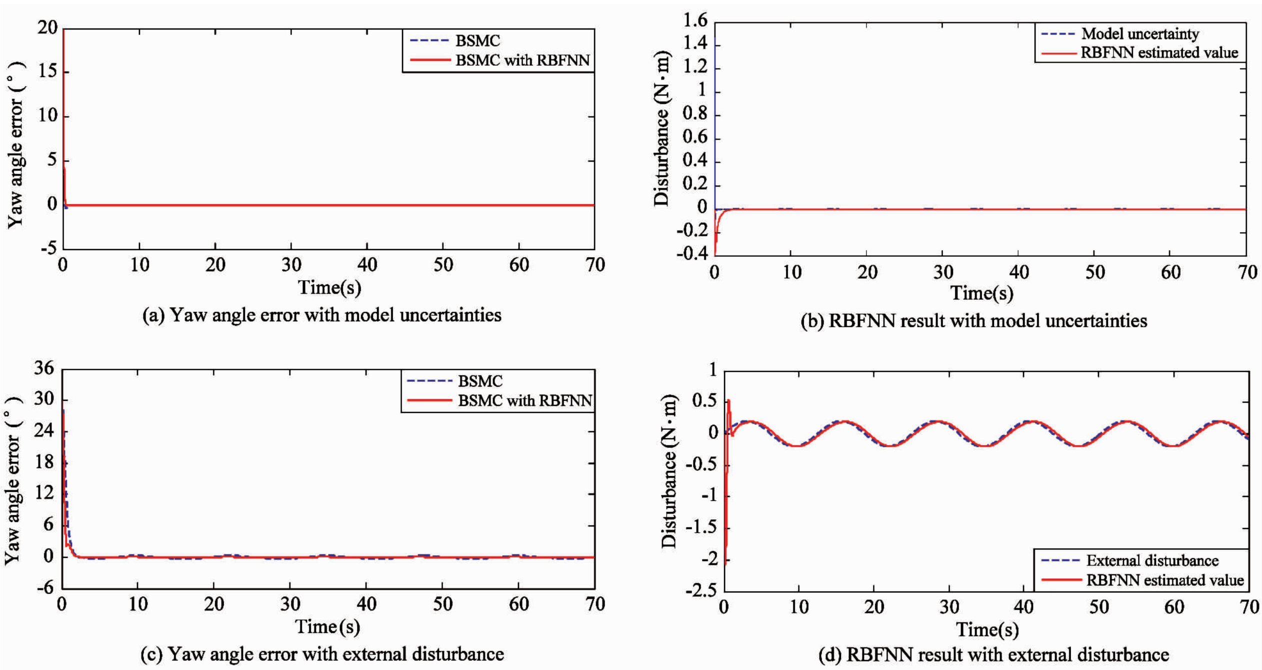

(a) Yaw angle error with model uncertainties

(b) RBFNN result with model uncertainties

(c) Yaw angle error with external disturbance

(d) RBFNN result with external disturbance

Fig. 6 The yaw control result with uncertainties

to see that the method proposed in this article has a better control performance than the BSMC, especially in the case of external disturbances. The overshoot of three attitude angle errors based on BSMC with RBFNN method under model uncertainties is all much smaller than those using BSMC method. Faced with external disturbance, the roll angle error with BSMC is limited in the range of ±0.056 °, whereas the roll angle error of BSMC with RBFNN is in the range of ±0.004 °. The pitch angle error using BSMC method is controlled in ±0.005 ° and it is limited at ±0.063 °. The yaw angle error is controlled in the interval of ±0.284 ° with BSMC, while it has the scope of ±0.012 ° using BSMC with RBFNN. In addition, the RBFNN observer has the satisfied uncertainties estimation performance. Through the comparison of the attitude simulation results, it can be seen that the coaxial twelve-rotor UAV has attractive control performance for the robust control problem under uncertainties and external disturbances.

4 Twelve-rotor prototype experiment results

4.1 Experiment setup

Fig. 7 is a prototype of the coaxial twelve-rotor UAV with a military level carbon fiber material, and twelve brushless direct current motors (BLDC) are installed at the end of each arm. Fig. 8 is a schematic diagram of the UAV flight control platform. TMS320F28335 DSP as the main controller can run at 150 MHz with

Fig. 7 The twelve-rotor prototype

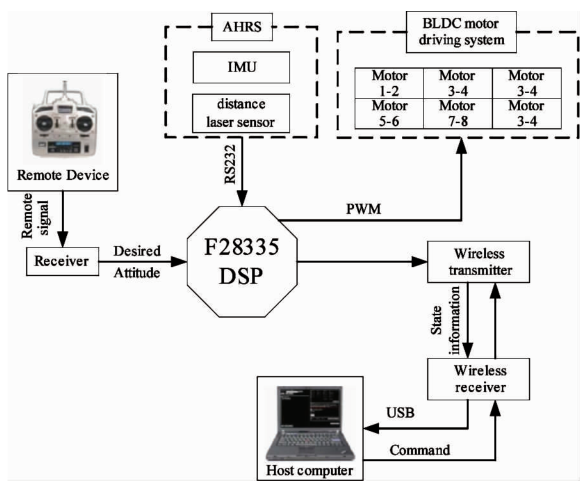

Fig. 8 The schematic view of aerial control platform

512 K flash memory, and support floating point calculations. The gyroscopes, magnetometers, accelerometers as well as the distance laser sensor form the inertial

measurement unit (IMU) to measure flight states. The sensor data are transmitted through an RS232 serial port to the flight control computer. Then, the data is sent back to the upper computer through the wireless transmission module and the corresponding schematic diagram is generated.

4.2 Experiment results

The twelve-rotor prototype experiment proves validity and robustness of BSMC and adaptive RBFNN algorithm. The parameters of the controller are set as the same as those in simulations. The desired attitude angles are taken by manual with remote device. The experimental environment has the wind disturbance whose speed is measured about 3.5 m/s with the anemometer. The three attitude control results are depicted in Fig. 9, Fig. 10 and Fig. 11, in which it can be seen that BSMC with RBFNN method has favorable attitude control performance and strong robustness.

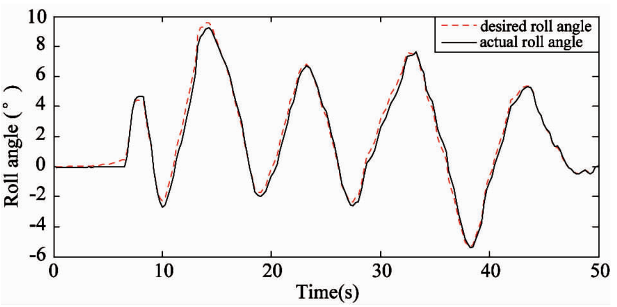

Fig. 9 The roll angle tracking result

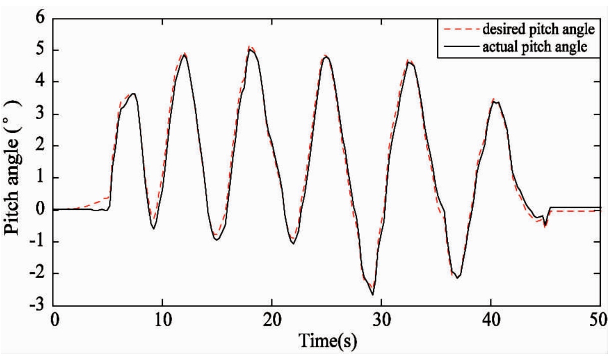

Fig. 10 The pitch angle tracking result

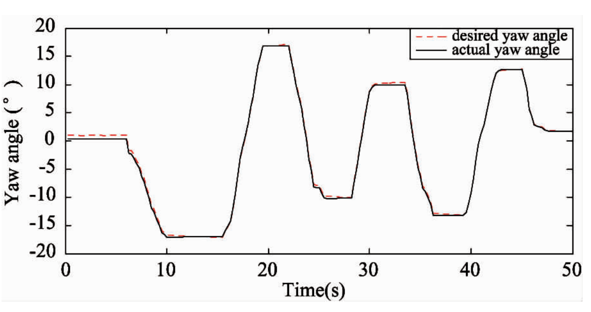

Fig. 11 The yaw angle tracking result

5 Conclusions

This paper designs a coaxial twelve-rotor UAV with stronger driving ability and motion attitude decoupling. On account of robust attitude control problem, the BSMC and RBFNN control strategy is targeted to deal with the uncertainty of the attitude control of the coaxial twelve-rotor UAV. The BSMC algorithm composed of backstepping and sliding mode control has prominent feature of simplified design procedure and increasing robustness. The adaptive RBFNN observer is able to estimate lumped uncertainties effectively. Eventually, simulation experiments verify BSMC with adaptive RBFNN control strategy applied to twelve-rotor UAV can provide favorable attitude control performance and strong robustness under model uncertainties and external disturbances. Meanwhile, the validity of the proposed method is verified again via coaxial twelve-rotor prototype tests.

Reference

[1] Ricardo P A, Javier M V, Roger M C. A robust approach for trajectory tracking control of a quadrotor with experimental validation. *ISA Transactions*, 2016, 65: 262-274

[2] Maravall D, de Lope J, Fuentes J P. Vision-based anticipatory controller for the autonomous navigation of an UAV using artificial neural networks. *Neuro-computing*, 2015, 151: 101-107

[3] Chen Z J, Zhang R L, Zhang P, et al. Flight control: chanllenges and opportunities[J]. *Acta Automatica Sinica*, 2013, 39(6):703-710(In Chinese)

[4] Mohammadi M, Shahri A M. Adaptive nonlinear stabilization control for a quadrotor UAV: theory, simulation and experimentation[J]. *Journal of Intelligent & Robotic Systems*, 2013, 72(1): 105-122

[5] Ryan T, Kim H J. LMI-based gain synthesis for simple robust quadrotor control[J]. *IEEE Transactions on Automation Science and Engineering*, 2013, 10(4): 1173-1178

[6] Derafa L, Benallegue A, Fridman L. Super twisting control algorithm for the attitude tracking of a four rotors UAV. *Journal of the Franklin Institute*, 2012, 349(2): 685-699

[7] Yeh F K. Attitude controller design of mini-unmanned aerial vehicles using fuzzy sliding-mode control degraded by white noise interference. *Control Theory Application IET*, 2012, 6 (9): 1205-1212

[8] Roger J S, Sun C T. Functional equivalence between radial basis function networks and fuzzy inference systems[J]. *IEEE Transactions on Neural Network*, 1933, 4(1): 156-159

Pei Xinbiao, born in 1990. He received his Ph. D degree from Univeristy of Chinese Academy of Sciences in 2018. He also received his B. S. degree from Jilin University in 2013. His main research direction is unmanned aerial vehicles integrated navigation and control.